Elsevier Editorial System(tm) for Bioresource Technology

Manuscript Draft

Manuscript Number: BITE-D-16-04258R2

Title: Structural changes of Arthrospira sp. after low energy sonication treatment for microalgae harvesting: elucidating key parameters to detect the rupture of gas vesicles

Article Type: Original research paper

Keywords: Arthrospira sp.; morphological/structural changes; low energy sonication treatment; gas vesicles rupture; microalgae harvesting monitoring.

Corresponding Author: Dr. Marti Lecina, PhD

Corresponding Author's Institution: Universitat Autònoma de Barcelona

First Author: Marti Lecina, PhD

Order of Authors: Marti Lecina, PhD; Benjamin Sanchez; Carles Solà; Jordi Prat; Monica Roldan; Hernandez Mariona; Ramon Bragos; Carlos J Paredes; Jordi J Cairo

Abstract: The buoyancy suppression by low energy sonication (LES) treatment (0.8W·mL-1, 20kHz,10s) has recently been proposed as an initial harvesting step for Arthrospira sp. This paper aims to describe the structural changes in Arthrospira sp. after LES treatment and to present how these structural changes affect the results obtained by different analytical techniques. Transmission electron microscopy (TEM) micrographs of trichomes evidenced the gas vesicles rupture but also revealed a rearrangement of thylakoids and more visible phycobilisomes were observed. Differences between treated and untreated samples were detected by confocal microscopy, flow cytometry and optical microscopy but not by electrical impedance spectroscopy (EIS). After LES treatment, 2-fold increase in autofluorescence at 610/660nm was measured (phycocyanin/allophycocyanin emission wavelengths) and a ten-fold decrease in side scatter light intensity (due to a reduction of trichome's inner complexity). This was further confirmed by optical microscopy showing changes on trichomes appearance (from wrinkled to smooth).

Highlights.

- Low Energy Sonication (LES) treatment suppresses *Arthrospira* sp buoyancy
- TEM images evidenced that loss of buoyancy was related to gas vesicles rupture
- TEM revealed structural changes after treatment, like circular-shaped thylakoids
- Structural changes can be detected by FACs, confocal and optical light microscopy

Structural changes of *Arthrospira* sp. after low energy sonication treatment for microalgae harvesting: elucidating key parameters to detect the rupture of gas vesicles

*Martí Lecina** [a], *Benjamin Sanchez* [b], *Carles Solà*[a], *Jordi Prat*[a], *Mònica Roldán*[c], *Mariona Hernández* [d], *Ramon Bragós*[b], *Carlos J. Paredes* [a] *and Jordi J. Cairó* [a]

[a] Department of Chemial, Biological and Environmental Engineering, Escola d'Enginyeria, Universitat Autònoma de Barcelona, 08193 Bellaterra, Spain.

[b] Electronic and Biomedical Instrumentation Group, Department of Electronic Engineering, Universitat Politècnica de Catalunya (UPC). Campus Nord, C-4. C/ Jordi Girona 1-3. 08034 Barcelona, Spain.

[c] Servei de Microscòpia, Universitat Autònoma de Barcelona, Edifici C, Facultat de Ciències, 08193, Bellaterra, Spain

[d] Dep. Productes Naturals, Biologia Vegetal i Edafologia. Facultat de Farmàcia, Universitat de Barcelona, Av. Joan XXIII s/n, 08028, Barcelona, Spain

(*) Corresponding author: marti.lecina@gmail.com

ABSTRACT

The buoyancy suppression by low energy sonication (LES) treatment (0.8W·mL^{-1}, 20kHz,10s) has recently been proposed as an initial harvesting step for *Arthrospira* sp. This paper aims to describe the structural changes in *Arthrospira* sp. after LES treatment and to present how these structural changes affect the results obtained by different analytical techniques. Transmission electron microscopy (TEM) micrographs of trichomes evidenced the gas vesicles rupture but also revealed a rearrangement of thylakoids and more visible phycobilisomes were observed. Differences between treated and untreated samples were detected by confocal microscopy, flow cytometry and optical microscopy but not by electrical impedance spectroscopy (EIS). After LES treatment, 2-fold increase in autofluorescence at 610/660nm was measured (phycocyanin/allophycocyanin emission wavelengths) and a ten-fold decrease in side scatter light intensity (due to a reduction of trichome's inner complexity). This was further confirmed by optical microscopy showing changes on trichomes appearance (from wrinkled to smooth).

17 **KEYWORDS**

18 *Arthrospira* sp.; morphological/structural changes; low energy sonication treatment;

19 gas vesicles rupture; microalgae harvesting monitoring.

20

1. INTRODUCTION

Microalgae production for nutritional applications has increased by 5-fold since the beginning of the 21st century (Ismail, 2010). Besides the increase of dried microalgae powder consumption, many industries have shown a growing interest in microalgae-based high-value molecules like pigments, fatty acids and anti-oxidants among others (Borowitzka, 2013; Vigani et al., 2015). Even more promising is the potential worldwide market of microalgae-derived biofuels (Mata et al., 2010), a technology which still needs some improvement. However, the need of processing large volumes of broth containing very low cell densities (Belay, 2013) is a barrier for the economic viability of such processes. It has been estimated (Grima et al., 2003) that between 20 to 50% of the total cost of microalgae production can be attributed to biomass harvesting and dewatering.

Microalgae harvesting efficiency is strongly linked to microalgae properties (basically cell surface charge, cell size and density) and consequently there is not a universal harvesting method for microalgae. While large cells can be harvested by filtration methods, sedimentation and centrifugation are normally adequate for cells with higher density than the culture media. Moreover, the use of flocculants (either by themselves or as part of air flotation t) facilitates microalgae harvesting of those species with densities more similar to the culture broth either by air flotation or sedimentation(Lecina et al., 2016). In other cases, this approach might be inefficient due to the presence of gas vesicles inside the cells (Walsby, 1972 and Pfeifer, 2012) and/or the production of an exopolymer, as occurs in *Arthrospira* sp.

cultures and in other cyanobacteria strains. Gas vesicles provide buoyancy whereas exopolymers can clog up filtration membranes quite fast and also can neutralize cell surface charges making ineffective the use of ionic flocculants.

One of the most important parameters used when comparing harvesting methods is the energy deposition. As a summary, Table I compiles different methods for microalgae harvesting and their estimated energy deposition. To address the high energy deposition required to harvest *Arthrospira* sp., we have recently described the use of a low energy sonication treatment that suppresses its buoyancy. This method preserves the cell integrity and viability (Lecina et al., 2015) and allows the use of sedimentation methods as a dewatering step.

Different applications of ultrasound treatments to microalgae cultures can be found in the literature as shown in Table II. Ultrasound treatment has been used to control blooms of toxic species (mainly *Microcystis aeruginosa*) in water reservoirs (Rajasekhar et al., 2012), as well as in cell disruption processes for the extraction of intracellular products (dos Santos et al., 2015). These treatments aim to either disrupt the cell or to suppress cell viability through the application of ultrasound with a frequency in the kHz range. Under such conditions the mechanism acting is called transient cavitation which consists in the creation of small bubbles that release a large amount of energy when collapsing. This sudden release of energy generates harmful effects on microalgae such as: cell growth inhibition, cell rupture (Hao et al., 2004), enzymes inactivation (Lee et al., 2001), damage of antenna complexes (Zhang et al., 2006) and photosystems resulting in a reduction of the

absorption peak of phycocyanin (Tang et al., 2003) and membrane breakage (Ahn et al., 2003) among others. If we compare the energy deposition of these methods with those of Table I it is clear that they are one order of magnitude higher. We refer to them as high energy sonication treatments based on their energy deposition.

The ultrasound treatment methods presented in Bosma *et al*. (Bosma et al., 2003) and Lecina *et al*. (Lecina et al., 2015) preserve cell integrity and viability although through different means. The ultrasonic cell separation presented in the former is based on applying frequencies in the MHz range in order to agglomerate cells in large aggregates that can sediment on their own. The energy deposition is significantly higher when comparing to the methods shown in Table I and on par with some of the high energy methods presented in Table II. The method presented by Lecina *et al.* uses ultrasounds in the kHz range and the mechanism is based on stable cavitation (low energy is generated from bubble resonance) (Mason, T.J. et al. 2002). The energy deposition of this method resulted in lower values than some of the centrifugation methods shown in Table I. When followed by a sedimentation step, the biomass harvesting yields reached values closer to 90% of total biomass recovery with an energy deposition about 1.1-2.2 kWh/m^3, while preserving cell viability.

However, there is no information about the effect of such low energy sonication treatment on *Arthrospira* sp. trichomes. In this sense, the paper describes the structural changes responsible for the suppression of buoyancy in *Arthrospira* sp.

after the low energy sonication treatment. Also the paper aims to describe how the results obtained by several analytical techniques were affected by the structural changes occurred after the treatment in order to evaluate the potentiality of those techniques to be applied for process monitoring in the future.

2. MATERIAL AND METHODS

2.1. Cyanobacteria strain and culture conditions

The *Arthrospira* sp. strain PCC8005 was used in this work. Cells were kept in an incubator with 1% CO_2 atmosphere and 95% of humidity (Forma scientific). Culture conditions were kept as follows: shaking rate of 100 rpm, a temperature of 35ºC and warm light (3000K) provided around the clock by LED (Light Emitting Diode) lamps at a photon flux of 54 µmol photons $m^2 \cdot s^{-1}$. Cells passaging and maintenance was performed once a week in 250mL shake flasks with Zarrouk medium using a 10-fold dilution rate.

The production of large volumes of *Arthrospira* sp. for experimental purposes was carried out in a 2-Liter photobioreactor (Sartorius Stedim, Germany) equipped with 2 marine impellers and a stirring rate of 200 rpm. The reactor was operated in continuous mode with a dilution rate of 0.03 h^{-1}. The pH was set at 9.5, it was monitored with a pH probe (Mettler Toledo) and controlled by CO_2 addition. The dissolved oxygen concentration was monitored using a polarographic electrode (Ingold) and maintained at 80% of saturation using a nitrogen-air mixture. LED lamps provided uninterrupted warm light at 405 µmol photons m^{-2} s^{-1}.

2.2. Low energy sonication treatment

Samples of 100 mL of volume were taken from the steady state of the 2L-bioreactor operating in continuous mode. Then samples were sonicated using an ultrasound homogenizer (Braun Labsonic 2000, Germany) at 20 kHz and room temperature. The ultrasound probe used was a Needle Probe (853811/5) of 127 mm of length and a diameter of 4 mm. The homogenization of samples for morphological studies required the use of a nominal sonication power of 80W for 10 seconds. Under this sonication conditions cells lose their buoyancy without any detrimental effect on cell integrity and viability.

2.3. Optical density

A bench spectrophotometer (Philips PU8620, Netherlands) was used to determine the optical density of samples. When needed, appropriate sample dilutions were performed to ensure that absorbance values were between of 0.1–0.9 AU at 530 nm (OD530).

2.4. Microscopy imaging

Live samples were mounted on Mat-Teck culture dishes (Mat Teck Corp., Massachusetts, United States) prior to their observation using a confocal spectral Fluoview1000 (Olympus, Tokyo, Japan) with a 60x (1.35 NA oil immersion) Universal Plan Apochromat Lens (UPlanApo) objective. Differential interference contrast (DIC) was visualized using the 488 nm excitation argon laser.

Autofluorescence from photosynthetic pigments was excited using the orange diode 559 nm (570-630 nm emission collected).

For measurements of emission spectra, a wavelength λ-scan function of the confocal microscopy was used. Images were acquired with the same objective. Photosynthetic pigments were excited with a 488 mm line of an Argon laser. Fluorescence emission was captured in 20 nm bandwidth increments (step size=10 nm) in the range 500 nm to 680 nm. A Region of Interest (ROI) in the thylakoid area was defined to determine Mean Fluorescence Intensity (MFI) in relation to the emission wavelength. Fluorescence measurements were expressed in arbitrary units (a.u.).

2.5. Transmission Electron Microscopy

Treated and non-treated samples were transferred to planchettes (3 mm diameter and 200 µm depth) and immediately cryo-immobilized using a Leica EM HPM 100 high-pressure freezer (Leica, Austria) and then stored in liquid nitrogen until further use. They were freeze-substituted over 3 days at –90 ºC in anhydrous acetone containing 2% osmium tetroxide and 0.1% uranyl acetate at –90 °C for 72 hours and warmed to room temperature, at 5 ºC per hour (EM AFS-2, Leica, Austria). After several acetone rinses in increasing concentrations of acetone, samples were infiltrated with Epon resin (Electron Microscopy Sciences, USA) during 2 days and flat embedded in a thin layer of resin and polymerized at 60 ºC during 48 h. Ultrathin sections were obtained using a Leica Ultracut UC6 ultramicrotome and mounted on Form var-coated copper grids. They were stained with 2% uranyl

acetate in water and lead citrate. Then, sections were observed in a JEOL 1010 TEM (Jeol, Japan) at 80 kV accelerating voltage.

2.6. Electrical Impedance Spectroscopy

The measurement system was based on an HP4192A impedance analyzer (Hewlett Packard, USA). The system was controlled by customized Labview (National Instruments, TX, USA) based software using an 82357B USB/GPIB interface. The impedance spectrum was measured with the four-electrode impedance technique performing a frequency sweep between 1 kHz and 10 MHz (10 frequency points per decade). Each measurement included an average of 10 sweeps. A customized front-end stage was used connected to the HP4192 to mitigate measurement errors. The technical details regarding the performance of the front-end can be found elsewhere (Sarro et al., 2012). Impedance measurements were calibrated using a baseline solution measurement so the frequency response of cables and electronics could be accounted for. The measurement cell was a PMMA prism (4cmx4cmx10cm) with four stainless steel (AISI316) rod electrodes at the bottom.

Starting from low energy sonication treated and non-treated samples at a concentration of 25 $g \cdot L^{-1}$, 5 consecutive 1:2 dilutions were prepared spanning a concentration range from 0.78 to 25 $g \cdot L^{-1}$. The two sets of six solutions each were then assessed by EIS. The resulting datasets were fitted to the Cole model (Equation 1) to obtain the Cole model parameters.

Impedance data was fitted to the Cole impedance model which is an empirical complex nonlinear function model in the (angular) frequency f.

$$Z(f,\theta) = R_\infty + \frac{R_0 - R_\infty}{1 + \left(j\frac{f}{f_c}\right)^\alpha},$$

Equation 1:

From the data fitting to the model, the theoretical values of impedance magnitude at a very low frequencies (i.e. $f \to 0$), R_0, at very high frequencies (i.e. $f \to \infty$), R_∞, the central relaxation frequency, f_c, and the α parameter could be obtained. The central relaxation frequency f_c, depends on the cell size and corresponds to the frequency with the highest absolute value of the impedance imaginary part. The α parameter corresponds to the depression of the Cole impedance arc away from a perfect semicircle shape (α =1) in the Cole plot, and takes into account the dispersion in the measured cellular membrane capacitances.

To prevent the interpretation of the biomass impedance measurements being influenced by temperature or conductivity variation effects, less sensitive estimators like phase angle at high frequency or relative variation of the impedance magnitude at low and high frequencies were used.

2.7. Flow cytometry

Relative size and cell structure complexity were analyzed by a cell flow cytometer Guava EasyCyte (Massachusetts, USA) equipped with two excitation lasers (blue

208 at 488nm and red at 640 nm). Forward scatter (FSC) and side scatter (SSC) were
209 collected in linear mode. A total cell count per analysis was fixed to 10000 events.
210 Cell density of both treated and non-treated samples was diluted to an optical
211 density (OD530) about 1. Data from flow cytometer measurements were analyzed
212 using GuavaSoft software provided by the vendor.
213
214 **2.8. Statistical analysis**
215 Numerical results are presented as the average of at least three independent
216 replicates (n=3). Error bars represents the standard deviation.
217 A paired Students' *t*-test was run in order to compare both sets of samples, before
218 and after the treatment. The outcome of the test was that the sets of samples were
219 significantly different with a p-value of 0.0056 ($p<0.05$).
220 The fitting to the Cole-Cole arc equation was performed following a complex (in the
221 sense of using complex numbers) non-linear fitting method that does not provide a
222 R^2 correlation coefficient, but a root mean square error which has not given values
223 above 5% in the worst case.

224 **3. RESULTS AND DISCUSSION**

225 Low energy sonication treatment ($0.8 W \cdot mL^{-1}$ for 10 seconds) was applied to
226 different *Arthrospira* sp. samples obtained from the steady state of a CST-PBR
227 (Continuous Stirred Tank Photobioreactor) in order to suppress microalgae
228 buoyancy. The outlet cell concentration of the CST-PBR was around 1 $g\ L^{-1}$
229 corresponding to the cell density in large scale photobioreactors. Treated samples

were analyzed by different techniques and compared to controls (non-treated samples)

3.1 Transmission Electron Microscopy (TEM)

Treated and non-treated samples were analyzed by transmission electron microscopy (TEM) in order to elucidate the changes in the cyanobacteria inner structure. No differences were observed either in the cell wall or in the cross walls and also the trichomes' size was comparable in both treated (T) and non-treated samples (NT). This confirmed the integrity of the cells after the low energy sonication treatment as suggested by our cell growth studies previously published (Lecina et al., 2015).

Three significant differences could be observed from the TEM micrographs between treated and non-treated samples. The first one concerns the morphology of the gas vesicles. In cyanobacteria (i.e. *Arthrospira*), gas vesicles are hollow cylindrical gas-filled structures of between 340 to 750 nm in length and 60 to 110 nm in width and they are responsible for providing buoyancy (Walsby, 1972, Pfeifer, 2012). In our case, their length and width can be clearly seen in the images, corresponding to the blackish longitudinal and circular sections within the trichomes in the orthogonal cuts of untreated cells (A, B and C), whereas only vesicles thin threads could be seen in treated cells (D, E and F). Longitudinal straight thylakoids and abundant gas vesicles can be observed into intrathylakoidal spaces in non-treated samples (B), while only curled bundles of thylakoidal membranes without gas vesicles can be seen in treated samples (E).

As recently reported (Dehghani, M. H. 2016 and cites therein) , the rupture of the gas vesicles is the cause of the loss of buoyancy of the treated cells. The second main difference was found in the arrangement of thylakoids within cells. In non-treated samples the gas vesicles are located into the cytoplasm between straight-shaped thylakoids, which changed to curled shaped around the location where gas vesicles were previously to the ultrasound treatment. Thirdly, phycobilisomes can be more clearly observed in the low energy sonication treated trichomes (G) compared to those trichomes from the control samples.

3.2 Confocal Microscopy

As the thylakoid membrane is the site of the light-dependent reactions of photosynthesis, confocal microscopy was used to assess if the large differences in thylakoid arrangement between treated and non-treated samples had any effect on the photosynthetic pigments fluorescence (Figure 1).

The treated aliquot showed that the photosynthetic system of cyanobacteria was not negatively affected by the ultrasounds treatment, since fluorescence of cells did not decrease. Actually, a 2-fold increase in phycobiliproteins fluorescence intensity of ultrasounds-treated samples was observed. In particular, the maximum autofluorescence was emitted by phycocyanin (PC, 610 nm) and allophycocyanin (APC, 660 nm).

These results differ from those published in other studies where higher energy sonication conditions were applied. The intracellular concentration of chlorophyll *a*

278 after ultrasounds treatment at 0.086 $W \cdot mL^{-1}$ for 16 minutes decreased differently
279 depending on the specie of microalgae studied, ranging from the 50% to 15% for
280 *Dunaliella salina* or *Nannochloropsis oculata* respectively (Joyce et al., 2014). The
281 decrease in fluorescence was attributed to a chlorophyll *a* leakage to the
282 extracellular medium as a result of cell disruption. Other authors observed an
283 increase in fluorescence of sonicated microalgae samples when measuring the
284 whole sample (intra- and extracellular fluorescence determined with a microplate
285 reader) (Wang et al., 2014). In other works it was suggested that cell disruption in
286 smaller fragments or cell wall rupture led to higher fluorescence measurements
287 (Gerde et al., 2012). However, it should be considered in the latter case that the
288 fluorescence emitted by soluble chlorophyll *a* released to the extracellular media
289 was not mitigated due to the overlapping effect of cells or cell fragments, what
290 might contribute to the higher fluorescence measured. Thus, an increase in
291 fluorescence would be expected when distinction between intra and extracellular
292 fluorescence was not taken into account. On the contrary, a series of papers have
293 reported a drop of chlorophyll *a* or intracellular fluorescence of many microalgae
294 species after ultrasound treatment. A treatment with an energy deposition of 26.67
295 kWh/m^3 (25 kHz, 0.32 W mL^{-1} for 5 minutes) led to a reduction of chlorophyll *a* by
296 21% and a PC (Phycocyanin) absorbance decrease about 45% while cell
297 concentration was only reduced by 10% in *M. aeruginosa* (Zhang et al., 2006).
298 Similar effects were found when high frequency ultrasound treatment (1.7 MHz, 0.6
299 W/cm^2 for 5 minutes, energy deposition not quantifiable) was applied to *Arthrospira*
300 *platensis* (Tang et al., 2003).
301

In the experimental conditions analyzed, since neither cell lysis nor cell disruption were observed in TEM micrographs (Figure S1), the fluorescence increase measured after low energy sonication treatment did not match any of the explanations presented above. Our hypothesis is related to thylakoids rearrangement that could lead to an effective increase of pigments fluorescence due to changes in the efficiency of photosystems. When both photosystems (I and II) are decoupled, part of the energy that the photosystem II transfers to the photosystem I through different photosynthetic pigments could emitted as fluorescence (Ector et al, 2012). Inman (Inman, 2004) showed that an ultrasound treatment resulted in a small but statistically significant reduction in chlorophyll *a* concentration, what would also explain the fluorescence increase observed in present study.

Finally, is worth mentioning that the emitted fluorescence of the photosynthetic pigments occurred in the red light spectra emission wavelengths which has usually been associated to healthy cells (Tashyreva et al., 2013). This is consistent with the high cell viability observed after low energy sonication treatment.

3.3 Optical light microscopy and flow cytometry analysis

Changes on cell morphology were also assessed by optical light microscopy. Non-treated cultures presented an internal roughness appearance, probably due to the gas vesicles being in the path of the light transmission. Treated cultures presented a smoother appearance since gas vesicles were suppressed.

The use of flow cytometry to monitor cell disruption or cell size reduction of *Scenedesmus dimorphus* after high energy sonication treatment has been previously reported (Wang et al., 2014). In flow cytometry, the forward scatter (FSC) light intensity (light the detector is located in line with the light beam) gives information about the particles size (cell volume), while the side scatter (SSC) light intensity is sensitive to inner inclusions or complexity of cells (cytoplasmic granules or the membrane roughness). Panels A and C on Figure 2 show the SSC vs FSC plots whereas panels B and D show the SSC histograms for non-treated and treated samples.

A certain heterogeneity in cell population distribution was observed in both cases in terms size (forward scatter plots). Such heterogeneity was expected due to the *Arthrospira* sp. morphology and structure. A single trichome of *Arthrospira* sp. is composed by multiple cells and hence trichome size can vary a lot. Nonetheless, a clear subpopulation was observed between 10^2 and 10^3 FSC axis units, representing the most abundant trichome size from the whole cell population. Much more interesting was the change on SSC values, where one order of magnitude drop can be observed after low energy sonication treatment (Figure 2D). Then, flow cytometry analysis was capable to detect the decrease in cell roughness or in number of inner cell complexes i.e. gas vesicles. These results corroborated the reduction of inner cell complexity due to the rupture of the gas vesicles observed under the microscope and were in good correlation to previous studies with *Microcystis* sp. (Jong Lee et al., 2000).

3.4 Electrical impedance spectroscopy (EIS)

Finally, non-treated and treated aliquots of *Arthrospira* sp. were analyzed by Electric Impedance Spectroscopy (EIS). Impedance spectroscopy studies have provided valuable information to estimate the evolution of cell concentration along cell culture expansion (De Blasio et al., 2004) and more recently, EIS has been applied to monitor morphological aspects of cells (Arndt et al., 2004 and Sarró et al., 2016). Therefore, it was expected that EIS could also provide information on the structural changes underwent by *Arthrospira* sp. after low energy sonication.

The effect of decreasing cell concentration for the two sets of six aliquots each, treated and non-treated with ultrasound, can be observed in the Cole impedance plots shown in Figure 3.

As it can be seen, EIS measurements were sensitive to cell density. The arcs decreased both in width and origin (R_0) with cell dilution. Only the R_0 parameter changed significantly between treated and non-treated samples, what was confirmed by running a paired Students' *t*-test with a p-value<0.05 (p=0.0056). The α value obtained for non-treated samples was 0.23, whereas its value was reduced to 0.19 after low energy sonication treatment. The fact that the obtained α values, which are associated to cell morphology properties, were smaller in the treated cultures indicated lower dispersion in cells morphology and/or in sizes distribution. It may indicate that gas vesicles could somehow interact with EIS measurements, but values were not considered different enough to truly state this observation. Additionally, the highest central frequency values for non-treated samples (57.3

374 kHz vs. 47.4 kHz) indicated a smaller apparent cell size of non-treated cells.
375 Apparently, this would be contradictory with the rupture of gas vesicles, since
376 bigger cell size would be expected for non-treated cyanobacteria cells when gas
377 vesicles were present in the cytoplasm.
378
379 Both the phase angle at high frequency (Figure 4 top) and the cell density
380 estimator based on relative variation between R_0 and R_∞ (not shown) provided
381 similar estimation of cyanobacteria concentration between low energy sonication
382 treated and non-treated samples. Nevertheless, the R_0 parameter is higher in non-
383 sonicated samples (Figure 4 bottom). This behavior is coherent with the fact that
384 gas vesicles increase the overall impedance, since vesicles are non-conductive,
385 but do not influence the viable biomass density, because the amount of
386 intracellular ionic solution surrounded by an insulating membrane is constant
387 regardless the presence of gas vesicles (Bragos et al.,1999). Biomass density
388 estimation through electrical impedance measurement is based on the fact that low
389 frequency electrical current cannot cross the cell membrane while high frequency
390 current can. If the viable cell density would change after sonication (i.e. membrane
391 breakage or cell lysis), the ratio between low and high frequency impedance, and
392 the associated phase angle at high frequency would also change (Soley et al.,
393 2005).
394
395 From the data obtained, it could be seen that cyanobacteria were not damaged
396 after treatment, thus the measurement of electrical impedance spectroscopy
397 responded in a similar way to viable cell concentration. Because of the low

accuracy at low cell densities, the use of cell density estimator had to be limited to cell densities higher than $1 g \cdot L^{-1}$. Although there is a difference between treated and non-treated samples in R_0, this parameter is also quite sensitive to medium conductivity and temperature being rather not suitable for gas vesicle density estimation in industrial measurements.

4. CONCLUSIONS

TEM images evidenced that the loss of buoyancy after low energy sonication treatment of *Arthrospira* sp. was related to gas vesicles rupture, but also revealed other structural changes after treatment like circular-shaped thylakoids. These overall changes affected the results obtained by some common analytical tools like confocal microscopy (fluorescence measurement), optical light microscopy and flow cytometry resulting in effective tools for directly/indirectly detect the rupture of gas vesicles and/or the structural changes after treatment without the need of TEM analysis. The use of such techniques should be explored in order to monitor the buoyancy suppression process.

SUPPLEMENTARY DATA

The following Supplementary data associated with this article can be found, in the online version: TEM images (Figure S1), Confocal microscopy images (Figure S2) and Optical light microscopy images (Figure S3).

ACKNOWLEDGMENTS

The project was supported by the Ministerio de Economia y Competitividad of the Spanish Government (INNPACTO, IPT-2012-0249-310000).

Arthrospira sp. strain (PCC8005) was kindly provided by Melissa project team at Autonomous University of Barcelona.

REFERENCES

1. Ahn, C.-Y., Park, M.-H., Joung, S.-H., Kim, H.-S., Jang, K.-Y., Oh, H.-M., 2003. Growth Inhibition of Cyanobacteria by Ultrasonic Radiation: Laboratory and Enclosure Studies. Environ. Sci. Technol. 37, 3031–3037.
2. Arndt, S., Seebach, J., Psathaki, K., Galla, H.-J., Wegener, J., 2004. Bioelectrical impedance assay to monitor changes in cell shape during apoptosis. Biosens. Bioelectron. 19, 583–594.
3. Belay, A., 2013. Biology and Industrial Production of *Arthrospira* (*Spirulina*), in: Handbook of Microalgal Culture. John Wiley & Sons, Ltd, pp. 339–358.
4. Bhave, R., Kuritz, T., Powell, L., Adcock, D., 2012. Membrane-Based Energy Efficient Dewatering of Microalgae in Biofuels Production and Recovery of Value Added Co-Products. Environ. Sci. Technol. 46, 5599–5606.
5. Borowitzka, M., 2013. High-value products from microalgae—their development and commercialisation. J. Appl. Phycol. 25, 743–756.
6. Bosma, R., van Spronsen, W., Tramper, J., Wijffels, R., 2003. Ultrasound, a new separation technique to harvest microalgae. J. Appl. Phycol. 15, 143–153.
7. Bragos, R., Gamez, X., Cairó, J.J., Riu, P. J. and Goida F. 1999. Biomass Monitoring Using Impedance Spectroscopy. Electrical bioimpedance methods: applications to medicine and biotechnology. Ann. New York Acad. Sci, 873, 299–305.
8. Danquah, M. K., Ang, L., Uduman, N., Moheimani, N., and Forde, G. M. 2009. Dewatering of microalgal culture for biodiesel production: exploring polymer flocculation and tangential flow filtration. J.Chem. Technol. Biotechnol., 84(7), 1078-1083.
9. De Blasio, B.F., Laane, M., Walmann, T., Giaever, I., 2004. Combining optical and electrical impedance techniques for quantitative measurement of confluence in MDCK-I cell cultures. Biotechniques 36, 650–663.
10. Dehghani, M. H. 2016. Removal of cyanobacterial and algal cells from water by ultrasonic waves—A review. J. Mol. Liq., 222, 1109-1114.
11. Dey, S., Rathod, V.K., 2013. Ultrasound assisted extraction of β-carotene from *Spirulina platensis*. Ultrason. Sonochem. 20, 271–6.
12. dos Santos, R.R., Moreira, D.M., Kunigami, C.N., Aranda, D.A.G., Teixeira, C.M.L.L., 2015. Comparison between several methods of total lipid extraction from *Chlorella vulgaris* biomass. Ultrason. Sonochem. 22, 95–9.

13. Ector, L., Hlúbiková, D., and Hoffmann, L. 2012. Preface: Use of algae for monitoring rivers. Hydrobiologia, 695 (1), 1-5.
14. Gerde, J.A., Montalbo-Lomboy, M., Yao, L., Grewell, D., Wang, T., 2012. Evaluation of microalgae cell disruption by ultrasonic treatment. Bioresour. Technol. 125, 175–81.
15. Grima, M.E., Belarbi, E.-H., Acién Fernández, F.., Robles Medina, A., Chisti, Y., 2003. Recovery of microalgal biomass and metabolites: process options and economics. Biotechnol. Adv. 20, 491–515.
16. Hao, H., Wu, M., Chen, Y., Tang, J., Wu, Q., 2004. Cavitation mechanism in cyanobacterial growth inhibition by ultrasonic irradiation. Colloids Surfaces B Biointerfaces 33, 151–156.
17. Inman D.A., 2004. Ultrasonic treatment of algae. Thesis. Cranfield University.
18. Ismail, A., 2010. Marine lipids overview: markets, regulation, and the value chain. Oilseeds fats Crop. Lipids 17, 205–208.
19. Jong Lee, T., Nakano, K., Matsumura, M., 2000. A new method for the rapid evaluation of gas vacuoles regeneration and viability of cyanobacteria by flow cytometry. Biotechnol. Lett. 22, 1833–1838.
20. Joyce, E.M., King, P.M., Mason, T.J., 2014. The effect of ultrasound on the growth and viability of microalgae cells. J. Appl. Phycol. 26, 1741–1748.
21. Lecina, M., Nadal, G., Solà, C., Prat, J., Cairó, J.J., 2016. Optimization of ferric chloride concentration and pH to improve both cell growth and flocculation in *Chlorella vulgaris* cultures. Application to medium reuse in an integrated continuous culture bioprocess. Bioresour. Technol. 216, 211–218.
22. Lecina, M., Prat, J., Paredes, C.J., Cairó, J.J., 2015. Non-disruptive sonication of *A. fusiformis (A. platensis*) cultures facilitates its harvesting. Algal Res. 7, 1–4.
23. Lee, T.J., Nakano, K., Matsumara, M., 2001. Ultrasonic Irradiation for Blue-Green Algae Bloom Control. Environ. Technol. 22, 383–390.
24. Mason, T. J. and Lorimer, J.P., 2002. “Applied sonochemistry.” The uses of power ultrasound in chemistry and processing. Wiley--VCH Verlag GmbH, Weinheim.
25. Mata, T.M., Martins, A.A., Caetano, N.S., 2010. Microalgae for biodiesel production and other applications: A review. Renew. Sustain. Energy Rev. 14, 217–232.
26. Mohn FH, 1980. Experiences and strategies in the recovery of biomass from mass cultures of microalgae., in: Shelef, G., Soeder, J. (Eds.), Algae Biomass. Elsevier, Amsterdam, pp. 547–71.

27. Pfeifer, F. 2012. Distribution, formation and regulation of gas vesicles. Nature Reviews Microbiology, 10(10), 705-715.
28. Rajasekhar, P., Fan, L., Nguyen, T., Roddick, F.A., 2012. A review of the use of sonication to control cyanobacterial blooms. Water Res. 46, 4319–29.
29. Sarró, E., Lecina, M., Fontova, A., Gòdia, F., Bragós, R., Cairó, J.J., 2016. Real time and on-line monitoring of morphological cell parameters using electrical impedance spectroscopy measurements. J. Chem. Technol. Biotechnol. 91, 1755–1762.
30. Sarro, E., Lecina, M., Fontova, A., Sola, C., Godia, F., Cairo, J.J., Bragos, R., 2012. Electrical impedance spectroscopy measurements using a four-electrode configuration improve on-line monitoring of cell concentration in adherent animal cell cultures. Biosens. Bioelectron. 31, 257–63.
31. Soley, A., Lecina, M., Gamez, X., Cairo, J. J., Riu, P., Rosell, X., Godia, F., 2005. On-line monitoring of yeast cell growth by impedance spectroscopy. J biotechnol., 118(4), 398-405.
32. Tang, J., Wu, Q., Hao, H., Chen, Y., Wu, M., 2003. Growth inhibition of the cyanobacterium *Spirulina (Arthrospira) platensis* by 1.7 MHz ultrasonic irradiation. J. Appl. Phycol. 15, 37–43.
33. Tashyreva, D., Elster, J., Billi, D., 2013. A novel staining protocol for multiparameter assessment of cell heterogeneity in Phormidium populations (cyanobacteria) employing fluorescent dyes. PLoS One 8, e55283.
34. Vigani, M., Parisi, C., Rodríguez-Cerezo, E., Barbosa, M.J., Sijtsma, L., Ploeg, M., Enzing, C., 2015. Food and feed products from micro-algae: Market opportunities and challenges for the EU. Trends Food Sci. Technol. 42, 81–92.
35. Walsby, A.., 1972. Structure and function of gas vacuoles. Bac. Rev. 36, 1–32.
36. Wang, M., Yuan, W., Jiang, X., Jing, Y., Wang, Z., 2014. Disruption of microalgal cells using high-frequency focused ultrasound. Bioresour. Technol. 153, 315–21.
37. Wiley, P.E., Campbell, J.E., McKuin, B., 2011. Production of Biodiesel and Biogas from Algae: A Review of Process Train Options. Water Environ. Res. 83(4), 326-338.
38. Zhang, G., Zhang, P., Liu, H., Wang, B., 2006. Ultrasonic damages on cyanobacterial photosynthesis. Ultrason. Sonochem. 13, 501–5.

Figure Captions

Figure 1. Spectral profile representing the mean fluorescence intensity spectra for *Arthrospira* sp. trichomes after treatment (T) and non-treated samples (NT). The maximum autofluorescence was emitted by PC (610 nm) and APC (660 nm). Scale bar = 5µm.

Figure 2. Flow cytometry analysis of treated and non-treated samples. Side scattered light vs. forward scattered light plots, and side scattering light histogram for non-treated *Arthrospira* sp. samples (A and B) and after low energy sonication treatment (C and D).

Figure 3. Cole impedance plot of non-treated (grey arcs) and after low energy sonication treatment (black arcs) of *Arthrospira* sp. samples at decreasing cell densities: ○, 25 g·L^{-1}; □, 12.5 g·L^{-1}; *, 6.25 g·L^{-1}; ▽, 3.13 g·L^{-1}; △, 1.56 g·L^{-1}; ◇, 0.78 g·L^{-1}.

Figure 4. Top: correlation between the cell density estimator based on phase angle at high frequency and real cell density values for non-treated (black circles) and after low energy sonication treatment (empty circles) of *Arthrospira* sp. aliquots. The range of cell density studied was from 0.39 to 25 g·L^{-1}. A linear correlation can be assumed for biomass density values higher than 1 g·L^{-1} for both sets of samples (non-treated and ultrasound-treated). Bottom: Evolution of the R0 parameter with cell density. R0 parameter values were higher for the non-treated

562 samples as a consequence of the presence of gas vesicles. Error bars
563 corresponds to the standard deviation of n=3 replicates.
564
565
566
567

Figure 1

Click here to download high resolution image

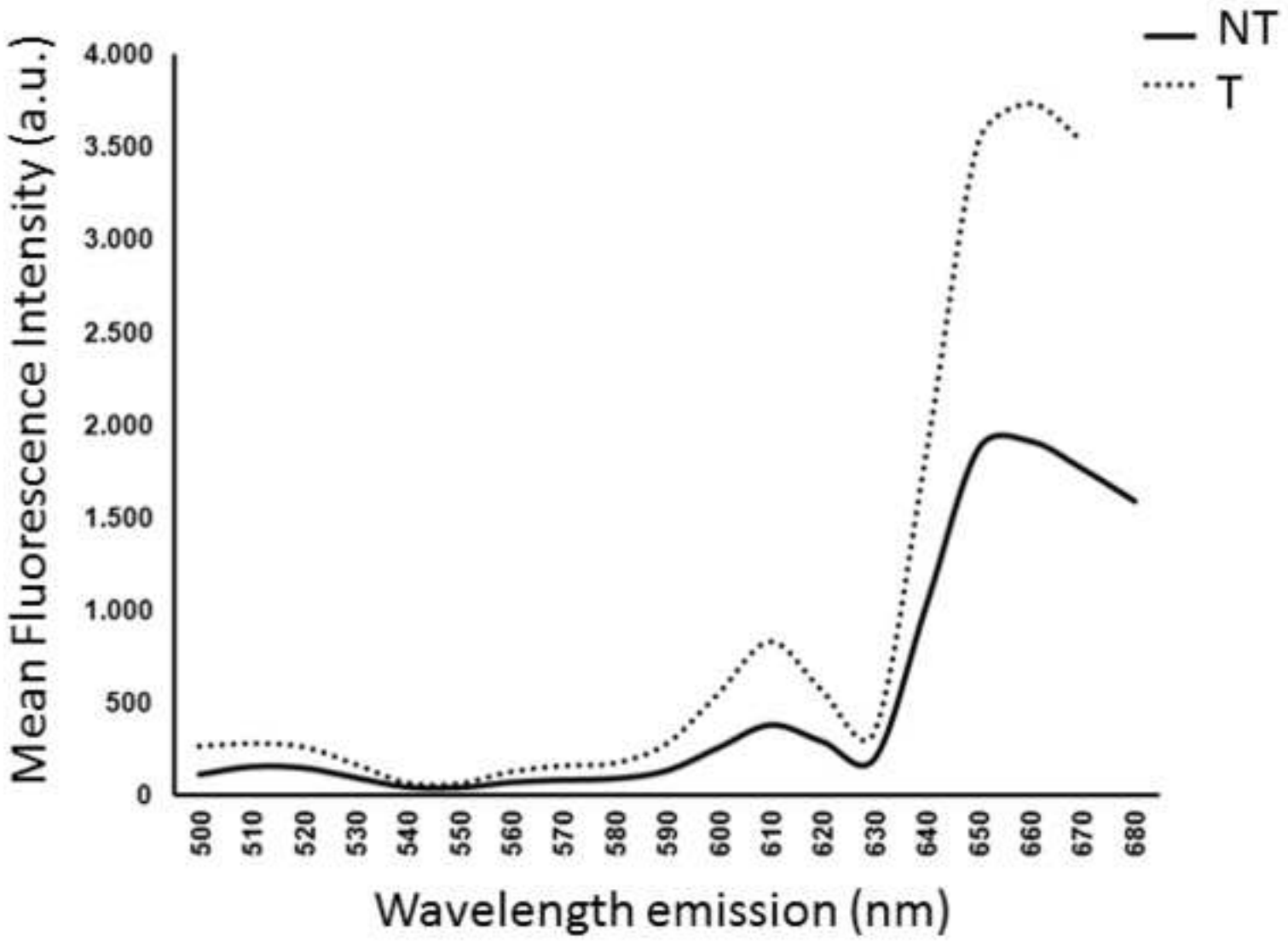

Figure 2

Click here to download high resolution image

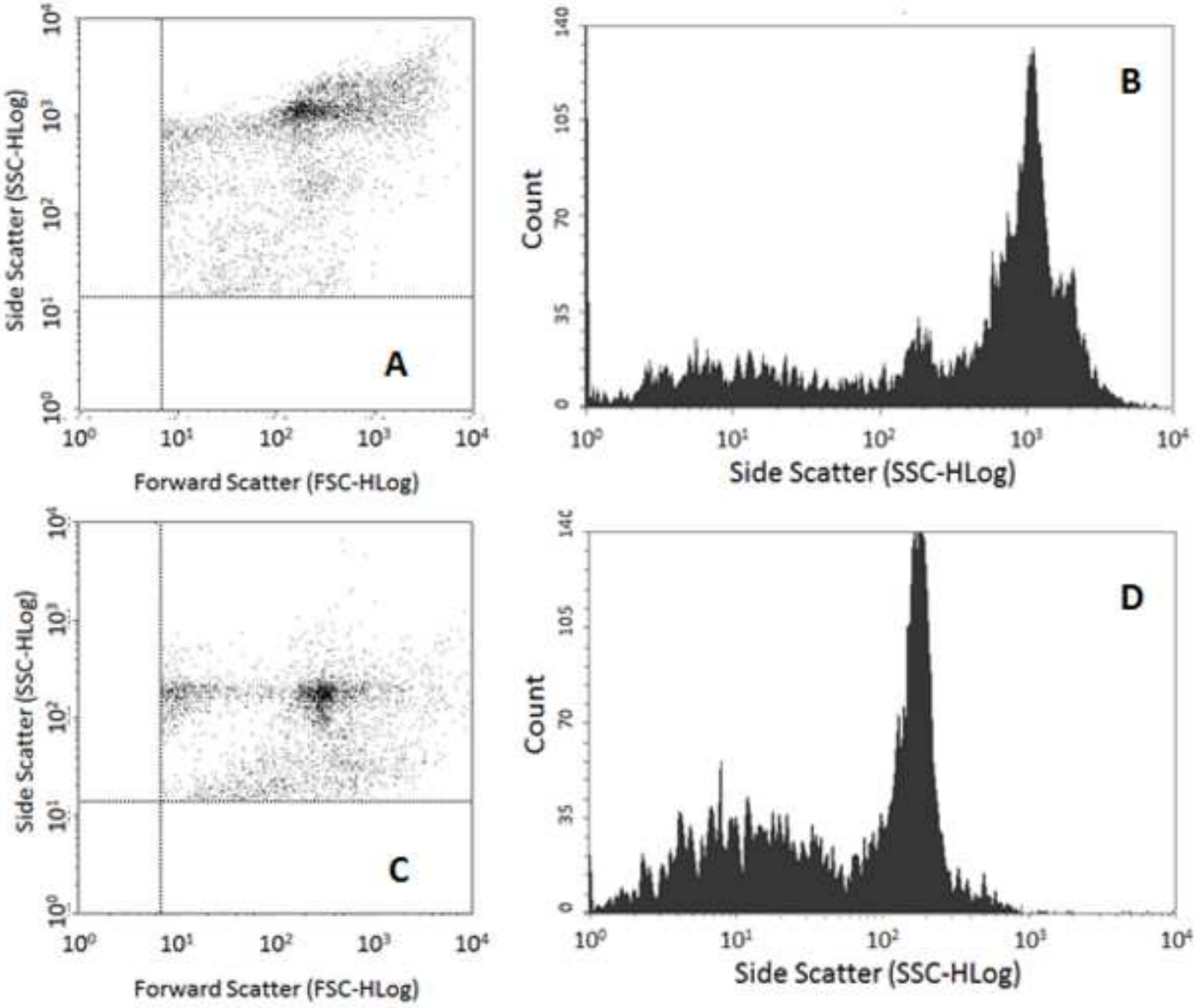

Figure 3

Click here to download high resolution image

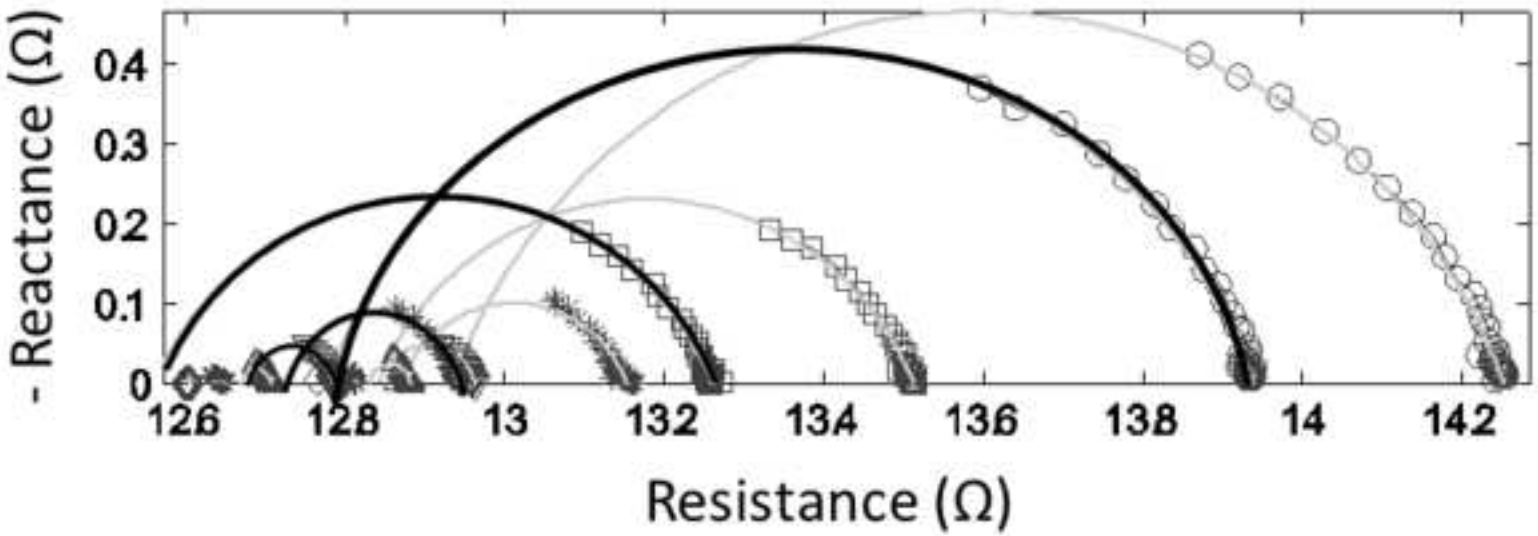

Figure 4

Click here to download high resolution image

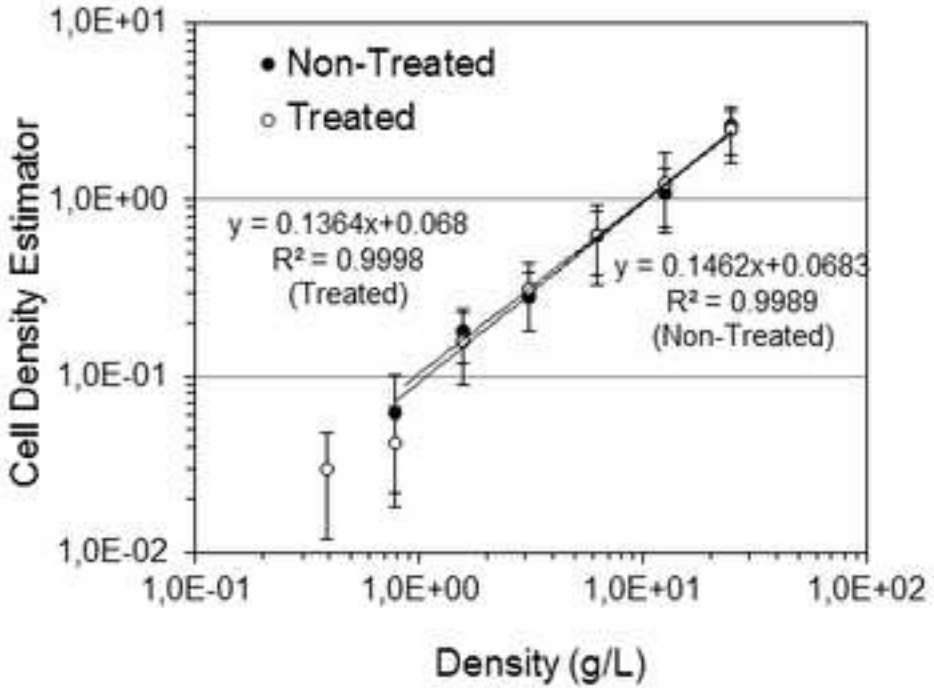

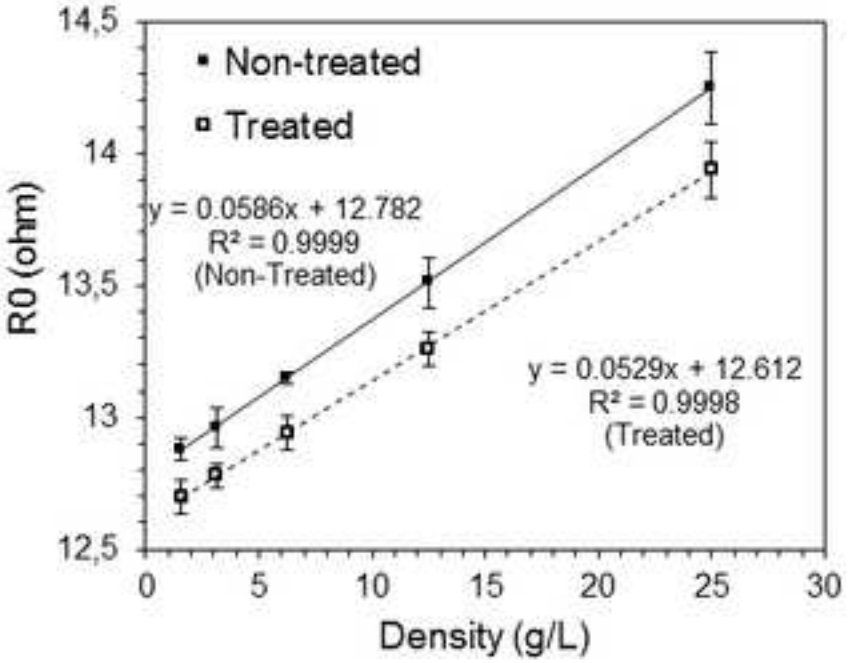

Table I

Table I: Compilation of different methods for microalgae harvesting and their estimated energy deposition. The energy deposition for centrifugation of *Arthrospira sp*. was obtained at 15000 rpm and inlet flow about 1.3 L/min as is provided for illustrative purposes.

Method	Microalgae	Energy deposition (kWh/m^3)	Reference
Centrifugation			
Disk stack	*Scenedesmus* sp., *C. proboscideum*	1	(Grima et al, 2003)
Decanter Bowl	*Scenedesmus* sp., *C. proboscideum*	8	(Grima et al, 2003)
Tubular Centrifuge	*Arthrospira* sp.	25.64	Present work
Filtration			
Chamber filter press	*C. proboscideum*	0.88	(Danquah M.K. et al, 2009, Mohn FH, 1980))
Tangencial Flow Filtration	*T. suecica*	2.06	(Danquah M.K. et al, 2009)
Crossflow Filtration	*Nannochloropsis* sp.	0.3-0.7	(Bhave, R. et al. 2012)
Dissolved Air Flotation	*Chlorella* sp., *Scenedesmus* sp.	7.6	(Wiley, P.E et al 2011)

Table II

Table II: Main features of different ultrasound treatments applications.

Method	Microalgae	Aim	Frequency	Energy deposition (kWh/m^3)	Mechanism	Reference
High energy sonication treatment	*Arthrospira platensis*	β-carotene extraction	20 kHz	214.8	Transient cavitation	(Dey S. et al., 2013)
	Microcystis aeruginosa	Cell growth inhibition (cell fracturing)	25 kHz	26.67		(Zhang G. et al., 2006)
	Chlamydomonas renhardtii	Cell disruption	20 kHz	22.2		(Gerde J.A. et al., 2012)
Ultrasonic separation	*Monodus subterraneus*	Cell aggregation	2.1 MHz	16-24	Induced aggregation	(Bosma R. et al.,2003)
Low energy sonication treatment	*Arthrospira* sp	Gas vesicles rupture	20 kHz	1.1 -2.2	Stable cavitation	(Lecina M. et al, 2015)

Suppl Figure S1

Click here to download Electronic Annex: Figure S1.tif

Suppl Figure S2

Click here to download Electronic Annex: Figure S2.tif

Suppl Figure S3

Click here to download Electronic Annex: Figure S3.TIF